26th International Congress of Mechanical Engineering
COBEM 2021
ABCM Associação Brasileira de Engenharia e Ciências Mecânicas
November 22-26, 2021, Virtual Congress, Brazil

COB-2021-1381
CFD ANALYSIS OF DIFFERENT COOLING ALTERNATIVES FOR A FSAE CAR BRAKE DISC

David Lelis Filho
Universidade Federal de Viçosa, Av. Peter Henry Rolfs, s/n - Campus Universitário, Viçosa - MG, 36570-000
david.filho@ufv.br

Júlio Cesar Costa Campos
Universidade Federal de Viçosa, Av. Peter Henry Rolfs, s/n - Campus Universitário, Viçosa - MG, 36570-000
julio.campos@ufv.br

Antonio Marcos de Oliveira Siqueira
Universidade Federal de Viçosa, Av. Peter Henry Rolfs, s/n - Campus Universitário, Viçosa - MG, 36570-000
antonio.siqueira@ufv.br

Marco Aurélio da Cunha Alves
Universidade Federal de Juiz de Fora, Rua José Lourenço Kelmer, s/n – São Pedro, Juiz de Fora - MG, 36036-900
marco.alves@ufjf.edu.br

Abstract. *The objective of this work is to develop a cooling analysis of the front brake disc of a formula SAE vehicle, comparing the behavior of different aerodynamic configurations, through the CFD method. The study of different disc cooling alternatives using CFD reduces prototyping costs, allows design changes more flexibly and reduces project development time, which is very beneficial for SAE projects. The methodology used was to compare four different aerodynamic configurations, one of the car without aerodynamic accessories, one with airfoils, another with a duct that takes air to the brake disc and finally one containing airfoils and the duct that takes air to the disc. Through wind tunnel simulations using ANSYS Fluent, for each aerodynamic configuration, the convection coefficient in the brake disc was obtained. Then, with the results of the transient thermal simulation, it was possible to compare the cooling time and evaluate the performance of each aerodynamic configuration. Concludes that the use of airfoils is more efficient in cooling compared to the configuration without aerodynamic accessories and the aerodynamic configuration that uses the duct that takes air to the disc is the one that promotes the greatest airflow in the inner region of the wheel, therefore it is the one that promotes more efficient cooling.*

Keywords: *Brake disc, CFD, formula SAE, ANSYS Fluent, convection coefficient, air duct.*

1. INTRODUCTION

A vehicle's brake system has the role of controlling its speed or keeping it stationary, which makes it possible to brake the vehicle before there is a possible collision, that is, its role is essential for safety. Keeping the temperature controlled in a brake system is essential for its proper functioning, as very high temperatures cause problems such as the formation of bubbles in the brake fluid, loss of friction, noise generation, irregular wear of the disc and pads, reduced component life, geometric deformation and thermal cracks (Breuer and Bill, 2004). Which in some cases leads to total system failure, making it impossible to brake the vehicle. Thus, the thermal study is necessary for a complete brake design.

The analysis using numerical methods brings advantages such as the possibility of solutions approximate for complex problems, which is not always possible in an analytical solution, which brings exact solutions, but limited to low complexity problems (Pandey, 2013). Furthermore, numerical methods were incorporated into computer simulations, optimizing the calculation process.

CFD (Computational Fluid Dynamics) is a type of numerical method that involves the study of fluid mechanics and heat and mass transfer problems, based on computer simulations. The use of this type of simulation reduces prototype development costs, allows changes to project more flexibly and reduces project development time. In addition, reliability of renowned commercial simulation program algorithms, such as ANSYS, is usually certified and validated through case studies that have results obtained analytically.

The general objective of this work is to develop a thermal analysis of the front brake disc of a formula SAE type vehicle, through the CFD method, in order to compare different aerodynamic configurations, for brake system cooling. Also, analyze the thermal performance of the brake disc, evaluate the fluid behavior and compare the cooling results obtained for each proposed aerodynamic configuration.

2. HEAT EXCHANGE IN THE BRAKE SYSTEM

According to Limpert (1999), the brakes must be designed so that the operating temperature is kept below a level that ensures the safe operation of system components. Furthermore, Milliken (1995) describes that the brake disc and the caliper must be adequately ventilated, with the air being directed to the center of the disc and, in case of problems with high temperature of the brake fluid, jets of air should be directed to the caliper.

Cooling air must be brought in from a high-pressure zone, for example from a geometry that precedes the brake system, such as a front airfoil. Some duct can also be used to carry this air, and to be effective, it must have a diameter of at least 76.2 mm, unless the duct is very short (Milliken, 1995).

According to Taborek (1957), the heat exchange in a brake system is done through conduction of the components from the friction surfaces (disc and pad), for the parts to which they are connected; radiation, that it reaches every brake system, however it depends on the absolute temperature; convection, which is responsible by the largest portion of heat exchange, and is influenced by the size and shape of the contact surface and by the velocity and turbulence of the air.

The heat generated in the disc brake at the friction contact interface is directly dependent on the work performed to stop the vehicle as defined by the local interface pressure, slip speed, friction contact and friction coefficient. These factors decide the type of distribution of pressure at the interface. However, during dynamic braking applications, the interface pressure is not uniform and changes with time, which causes a combination of mechanical distortions, thermal distortions and wear at the interface (Afzal and Mujeebu, 2018).

Limpert (1999) describes that the braking energy (E_b) in a vehicle, from the start of braking until its stop, considering that all rotating components are expressed in relation to the wheel rotation, is given by:

$$E_b = \frac{kmV^2}{2} \tag{1}$$

Where k is the correction factor for rotating masses, given by:

$$k \approx 1 + \frac{I}{R^2 m} \tag{2}$$

Where R is the radius of the tire [m]; m the vehicle mass [kg]; I the moment of inertia for rotating parts [kg.m²] and V the speed at the beginning of braking [m/s].

Gillispie (1992), considers that it can be assumed that the forces acting during the braking of a vehicle are constant, so we have that the stopping time of the car (t_s), will be the ratio between the speed at the start of braking (V) and acceleration (a):

$$t_s = \frac{V}{a} \tag{3}$$

The braking power (P_b) is calculated by the ratio between the braking energy Eq. (1) and Eq. (2), and the time of braking Eq. (3). So, the power can be calculated by (Limpert, 1999):

$$P_b = \frac{kmaV}{2} \tag{4}$$

Through the calculated power Eq. (4), the heat flux (q_o") generated on the friction surface of the disc:

$$q_o" = \frac{P_b}{A_s} \tag{5}$$

Where A_s is the friction surface area.

This braking power, calculated by Eq. (4), is the total power needed to stop the vehicle completely, and this power is not distributed equally throughout the entire brake system of the car. So, due to load transfer during braking, the front brakes are more required than the rear ones, that is, by Eq. (5) it is noted that the front brake will have greater heat input and consequently a higher temperature than the rear (Limpert, 1999).

For the calculation of the convection coefficient, for a solid disc we have (Limpert, 1999):

$$h = \begin{cases} 0.7 \left({k_a}/{d_{out}} \right) Re^{0.55}, \; Re \leq 2.4 \times 10^5 \\ 0.4 \left({k_a}/{d_{out}} \right) Re^{0.8}, \; Re > 2.4 \times 10^5 \end{cases} \tag{6}$$

Where k_a is the thermal conductivity of air, 0.0267 W/m.K; d_{out} the outer diameter of the disc [m] and Re Reynolds number, which is given by:

$$Re = \frac{V \rho_a d_{out}}{\mu_a} \quad (7)$$

Where V is the car speed [m/s]; ρ_a is the air density, 1165 kg / m³ and μ_a the air viscosity, 1.8×10^{-5} Pa.s.

Equations (6 and 7) were obtained by experimental data collected in a brake disc system of a light truck (Limpert, 1999).

3. METHODOLOGY

3.1 Analyzed geometries and mesh

The analyzed geometry has 4 different aerodynamic configurations, one of the car without aerodynamic accessories, one with only airfoils, another with only a duct that takes air to the front brake disc and a geometry containing airfoils and the duct takes air to the disc (Figure 1).

Figure 1. Formula vehicle geometry with airfoils and duct that takes air to the brake disc.

The brake disc geometry is the same for the 4 types of configurations and has 220 mm of outer diameter. In addition, the duct highlighted in Figure 1 that brings air to the front brake disc, is designed with a diameter of 80 mm, given the minimum diameter of 76.2 mm recommended by Milliken (1995), and it is located so that its air outlet nozzle is aligned with the center of the disc and points towards the front region of the inner part of the wheel.

In order to facilitate the mesh creation process, reduce the computational demand, some parts of the car's geometry were not included, such as suspension arms, wing supports and suspension springs. Other parts like the rear wheel, pilot and axle sleeve were designed in a simplified way. Furthermore, as this is a symmetric problem, it will be simplified using only half of the car.

To measure the quality of the tetrahedral mesh, skewness was evaluated, which determines how much near ideal an element or element face is. Using the average and maximum skewness data, meshes were created with average skewness below 0.25 which, according to Ansys (2019), are values excellent, in addition to keeping the maximum skewness within an acceptable value.

3.2 Turbulence models

Turbulence models have the function of simulating the effect of turbulence on fluid behavior, while leaving the details of the turbulent structure in the background; determine a set of universal constants, which will be applied to the widest possible range of problems; build one curve fitting procedure to achieve the desired result (Abbott and Basco, 1989). The main models are:

The Spalart-Allmaras model, which is a relatively simple model, having only one equation that solves the transport equation for turbulent viscosity kinematics. It is also a low Reynolds number model, requiring the region affected by the boundary layer viscosity be properly resolved (Askari *et al*., 2011).

The k-ε model is the most used in the CFD industry, as it presents characteristics such as robustness, computational economy and good results for a wide range of problems, which makes it popular in the industry in general (Belhocine and Omar, 2018).

The k-ω model does not have the same computational economy as the k-ε, but it has robustness and best results for problems with adverse pressure gradients and boundary layer separation.

SST is a calibrated model to accurately predict fluid separation from smooth surfaces and, is one of the most used models in simulations where aerodynamic data such as gradients of pressure and velocity profiles are desired (Igali *et al.*, 2019).

Thus, for the turbulence model, the k-ε realizable model was selected, as it is widely used in industry, have lower computational cost compared to the SST model and have good results for this type of simulation. As evidenced by Vidiya and Singh (2017) in his work, that performing a thermal analysis of a FSAE vehicle brake disc and comparing with experimental results.

3.3 Boundary conditions

Boundary conditions were defined for the control volume, shown in Figure 2, according to Guerrero and Castilla (2020). This figure has the following definitions:

• Inlet - indicates the speed at which the car travels immersed in the working fluid (air), the selected speed was 48 km/h, as it is the average speed developed in the race that most demands of the vehicle in FSAE competition according to SAE (2019);

• outlet - where the relative pressure is zero, as the pressure outside the control volume is equal the pressure within the control volume (atmospheric pressure);

• walls - are areas where the air does not pass through, with slip condition;

• symmetry - face where the total geometry was halved for simplification;

• brake disc - located in the inner region of the wheel, having a rotation speed of 53.83 rad/s, like the wheel.

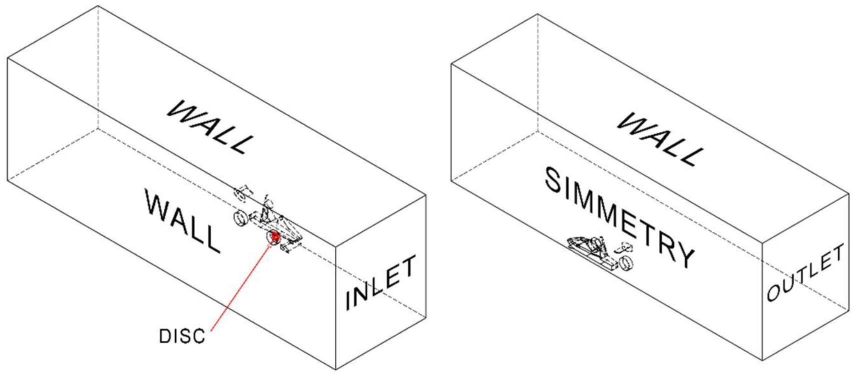

Figure 2. Control volume and its boundary conditions.

Due to air turbulence the ends of the control volume must be at a certain distance from the car. Distances were selected according to Guerrero and Castilla (2020), with an additional distance on the side and top walls. Thus, the distances are 5 times the length of the car, from front to air inlet, 8 times its length, from rear to outlet, 5 times the height of the car from its highest point to the top wall and 5 times the width from the side of the car to the side wall. Based on these recommendations, Figure 3 was elaborated for this study.

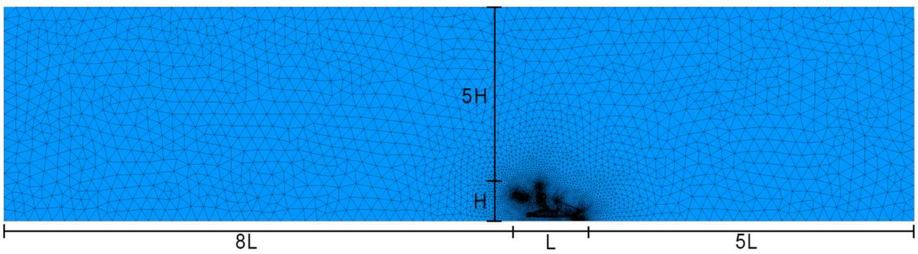

Figure 3. Measures used in the control volume.

3.4 Transient thermal simulation

The brake disc thermal transient problem has two main boundary conditions, the input of heat generated during braking by friction between the disc and the pad and the heat transfer caused by convection on the free surfaces of the disc (Belhocine and Bouchetara, 2011).

The thermal boundary condition is mainly given by heat transfer by convection and radiation. Since the heat transfer by radiation in the sudden braking process is not very important, and accurate calculation of radiation is complex, so the influence of thermal radiation is disregarded (Jian and Shui, 2017).

For this work, the time after the heat was generated by friction was considered, thus, after performing the wind tunnel simulation in Fluent, the convection coefficient values generated by each aerodynamic configuration were obtained, then, this value of convection coefficient, together with the temperature of the brake disc after braking, are the input values for the thermal transient simulation of the disc.

According to Belhocine and Bouchetara (2011), the heat generated by friction causes the brake disc temperatures, after braking, range from 300°C to 800°C. In a SAE formula type vehicle this temperature ranges from 300ºC to 550ºC during the endurance race, as evidenced by Vidiya and Singh (2017).

The analyzed disc is made of AISI 1045 steel, which has a density of 7850 kg/m³, thermal conductivity of 49.8 W/mK and specific heat of 486 J/kg.K. Furthermore, the analysis was performed over 25 seconds with an initial temperature of 550ºC and the convection coefficient obtained on the simulation before.

4. RESULTS

Using the calculation described by Limpert (1999) Eq. (6 and 7), considering a solid disc with an external diameter of 220 mm and car speed of 13.33 m/s, we have that the convection coefficient is equal to 66.94 W/m².K. While for the simulation performed in Fluent, the convection coefficient in the disc generated by air at 25ºC, with the car at 13.33 m/s is shown in Table 1:

Table 1. Simulation data for each aerodynamic configuration.

Car without aerodynamic accessories							
Mesh	Number of elements	Average skewness	Iterations to converge (RMS < 1x10^-3)	Drag coefficient	Diff (%)	Convection coefficient [W m^-2 K^-1]	Average [W m^-2 K^-1]
1	2097406	0.214	1066	39.668		52.780	53.506
2	2713530	0.213	941	38.967	1.767	54.235	Standard deviation
3	3252913	0.213	820	39.416	1.152	53.042	
4	3868081	0.212	872	39.383	0.084	53.968	0.704
Car with airfoil only							
Mesh	Number of elements	Average skewness	Iterations to converge (RMS < 1x10^-3)	Drag coefficient	Diff (%)	Convection coefficient [W m^-2 K^-1]	Average [W m^-2 K^-1]
1	5972610	0.214	796	64.321		68.608	68.646
2	6685735	0.213	860	62.561	2.736	70.587	Standard deviation
3	7141993	0.213	836	64.319	2.810	67.430	
4	7781555	0.213	840	62.866	2.259	67.958	1.381
Car with air duct only							
Mesh	Number of elements	Average skewness	Iterations to converge (RMS < 1x10^-3)	Drag coefficient	Diff (%)	Convection coefficient [W m^-2 K^-1]	Average [W m^-2 K^-1]
1	3770116	0.213	852	40.318		89.142	88.270
2	4397927	0.220	984	40.542	0.556	87.613	Standard deviation
3	4911594	0.220	836	41.562	2.516	87.953	
4	5492930	0.212	952	40.888	1.622	88.373	0.659
Car with airfoil and air duct							
Mesh	Number of elements	Average skewness	Iterations to converge (RMS < 1x10^-3)	Drag coefficient	Diff (%)	Convection coefficient [W m^-2 K^-1]	Average [W m^-2 K^-1]
1	7053255	0.213	718	63.787		85.058	85.082
2	7657587	0.213	864	63.186	0.942	85.239	Standard deviation
3	7963165	0.213	730	63.194	0.013	85.498	
4	8213176	0.213	786	63.950	1.196	85.015	0.106

From Table 1, it is observed that, for the simplest geometry (without aerodynamic accessories) it was possible to obtain a difference of 0.084% between the drag coefficient of the last two meshes, as for the more complex geometries (with some type of aerodynamic accessory), it was not possible to obtain a difference close to this value, as there was an increase in the complexity of the mesh, which generates a higher computational1 cost for the simulation, so due to computational limitations, the number of mesh elements was limited. Even with this limitation, for the other 3 geometries, it was possible to obtain a difference of less than 2.3 % between the drag coefficient results of the last two meshes. As for the convection coefficient, which is the variable of interest, a minimum standard deviation of 0.11 and a maximum of 1.38, was obtained between the studied meshes.

Table 1 shows that the result of the convection coefficient obtained by calculating Eq. (6) was closer to the coefficient of the car with airfoils and without the air duct, with a difference of 3%. As Eq. (6) was obtained with experimental data from a light truck for a solid brake disc, differences are expected, mainly in relation to the aerodynamic configurations that use the air duct, since it has the objective of forcing the circulation of air around the disc.

The greater the air flow promoted in the region of the brake disc, the greater the convection generated, therefore, the aerodynamic configuration that has the lowest convection coefficient value is the one that does not have aerodynamic accessories, with a convection coefficient of 53.51 W/m².K (Table 1), as it has no means of forcing air circulation in the inner region of the wheel. While the configuration which has the highest convection coefficient is the one containing the air duct, as it takes air directly to the brake disc, obtaining a value of 88.27 W/m².K for the car with only the duct and 85.08 W/m².K for car with duct and airfoils.

This difference between the air flow promoted by the car with and without a duct can also be noticed by the velocity vectors shown in Figure 4:

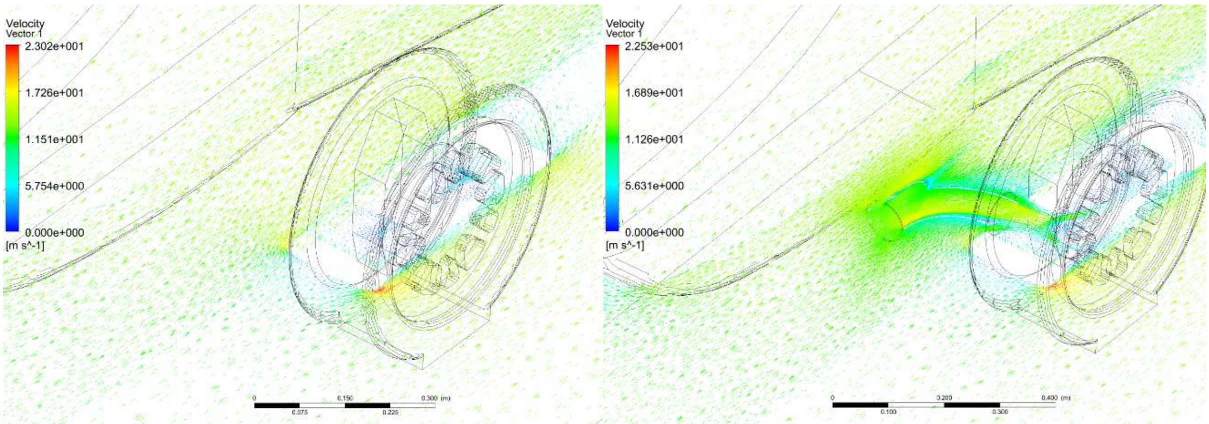

Figure 4. Comparison between airflow of geometries with and without the duct.

It is also interesting to note that the configuration with airfoil and without duct promoted a greater airflow than the airfoil and without duct configuration, with a difference of 15.14 W/m².K, due to characteristic of the airfoil to generate vortices by altering the airflow through the car.

In addition, the configuration with airfoil and duct achieved a 3.5% convection coefficient smaller than the configuration only with duct, as the airfoil generated an air deceleration in the region that precedes the air duct, as shown in Figure 5:

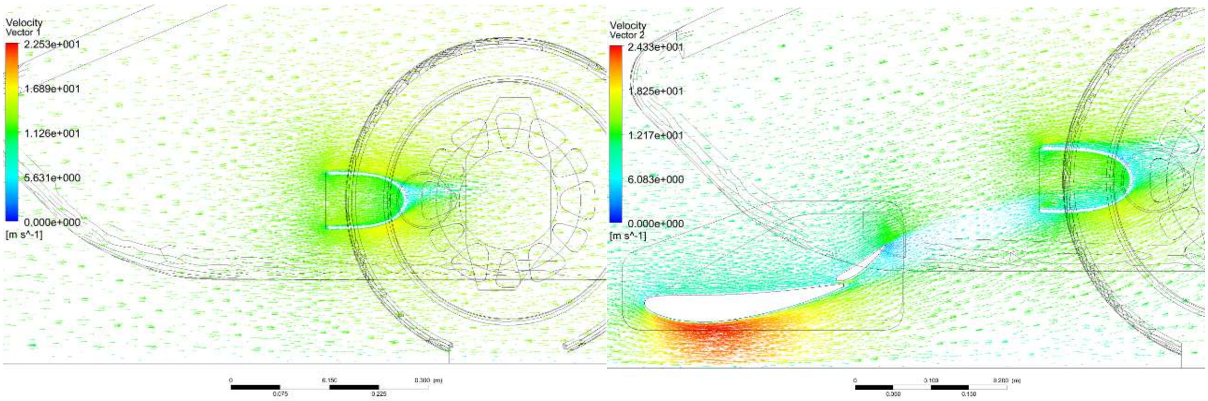

Figure 5. Comparison between airflow entering the duct with and without airfoil.

With the convection values in Table 1, the cooling curve of the brake disc over 25 seconds was obtained through thermal transient simulation. The simulation was done with a mesh of 134958 hexahedral elements, 25 steps of 1s and 13 substeps, for each of the 4 aerodynamic configurations, shown in table 2:

Table 2. Transient simulation data for each aerodynamic configuration.

	Car without aerodynamic accessories	Car with airfoil only	Car with air duct only	Car with airfoil and air duct
Convection coefficient	53.506	68.646	88.270	85.082
Initial temperature (Cº)	550	550	550	550
Final temperature (Cº)	460.443	437.467	410.532	414.765

The Table 2 and Figure 6 shows the difference between the average disc temperature of each aerodynamic configuration, in which it is noted that the difference between the temperatures of the configuration of the car with only the air duct (final temperature of 411ºC) and with airfoils and air duct (final temperature of 415ºC) is only 4 degrees after 25 seconds. While for the car without aerodynamic accessories (final temperature of 460ºC), after 25 seconds, there is a difference of 23 degrees in relation to the car with airfoils (final temperature of 437ºC) and 49 degrees in relation to the one with the air duct.

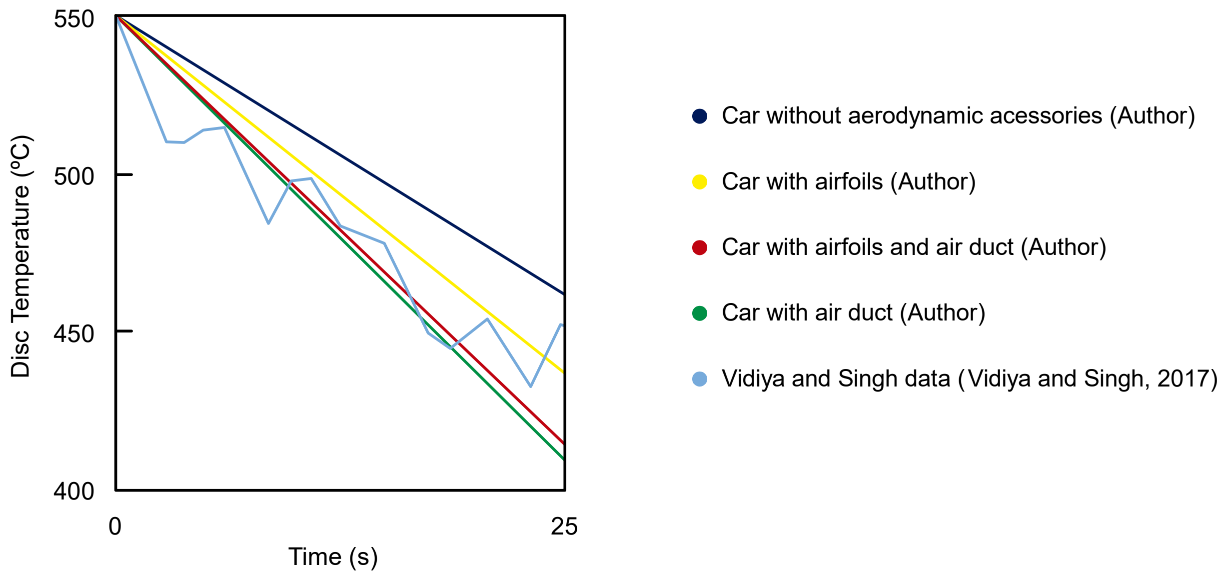

Figure 6. Comparison between average disc temperature for each aerodynamic configuration and Vidiya and Singh (2017) data.

The data found by Vidiya and Singh (2017), is a graph of the brake disc temperature variation over 8 laps of the endurance track of the formula SAE competition, and his data in Figure 6 is the part of the graph plotted by Vidiya and Singh (2017) after a 550ºC peak and before another temperature peak.

The study carried out by Vidiya and Singh (2017) was also carried out on a formula SAE car that uses airfoils, which makes the comparison in Figure 6 interesting, as similar values are expected. At the main differences found are in relation to the type of chart, while data from Vidiya and Singh (2017) were collected for the speed variations along the endurance track, the author data are in relation to the average speed on the endurance track, but the drop in temperature over the time studied remained similar.

The temperature distribution along the disc for the car with airfoils and air duct is displayed in Figure 7, the highest temperatures being located near the center of the disc and the temperatures located on the outer region of the disc. For other aerodynamic configurations the regions of high and low temperature remained similar.

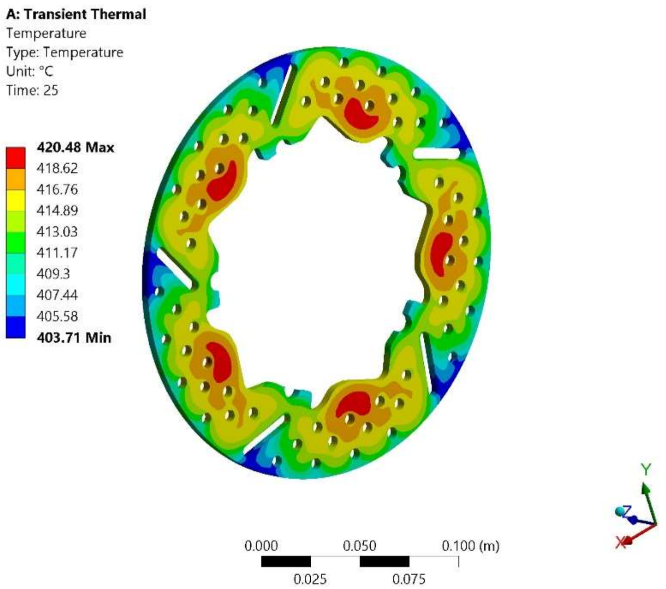

Figure 7. Temperature distribution on the brake disc for the car with airfoil and air duct.

5. CONCLUSION

The use of the air duct proved to be really effective in bringing air to the disc, promoting a greater decrease in the temperature of the brake disc, with values of up to 50 ºC lower compared to a car without aerodynamic accessories. Furthermore, the use of airfoils also proved to be more efficient in cooling compared to the configuration without aerodynamic accessories, with a difference of 23 ºC after 25 seconds.

The combination using the duct with airfoils generated a slight drop in airflow in the disc region compared to the use of the duct alone, which, despite not having resulted in significant differences, indicates that there is a need to optimize the use of these accessories together. So that the air duct inlet does not coincide with the low pressure zone, but with the high pressure generated by the front airfoil. Another complementary study would be in relation to the change in the drag of the car generated by the use of the air duct.

In conclusion, for application in the SAE formula project, the use of an air duct increases the life of the brake system components, resulting in greater safety for the vehicle and preventing failures in the brake system during the endurance race, which is essential for the FSAE competition.

6. REFERENCES

ABBOTT, M.B.; BASCO, D.R. **Computational Fluid Dynamics: an introduction for Engineers**. Longman, 1989.

AFZAL, Asif; MUJEEBU, Muhammad Abdul. Thermo-Mechanical and Structural Performances of Automobile Disc Brakes: a review of numerical and experimental studies. **Archives Of Computational Methods In Engineering**, [S.L.], v. 26, n. 5, p. 1489-1513, 3 set. 2018. Springer Science and Business Media LLC. http://dx.doi.org/10.1007/s11831-018-9279-y.

ANSYS, Inc. **Workbench User‘s Guide**. 19.0: ANSYS, 2019. Disponível em: https://ansyshelp.ansys.com/. Acesso em: 26 nov. 2019.

ASKARI, S.; SHOJAEEFARD, M.H.; GOUDARZI, K.. Numerical and analytical solution of compressible flow over double wedge and biconvex airfoils. **Engineering Computations**, [S.L.], v. 28, n. 4, p. 441-471, 31 maio 2011. Emerald. http://dx.doi.org/10.1108/02644401111131885.

BELHOCINE, Ali; BOUCHETARA, Mostefa. Thermal analysis of a solid brake disc. **Applied Thermal Engineering**, [S.L.], v. 32, p. 59-67, jan. 2012. Elsevier BV. http://dx.doi.org/10.1016/j.applthermaleng.2011.08.029.

BELHOCINE, Ali; OMAR, Wan Zaidi Wan. CFD analysis of the brake disc and the wheel house through air flow: predictions of surface heat transfer coefficients (sthc) during braking operation. **Journal Of Mechanical Science And Technology**, [S.L.], v. 32, n. 1, p. 481-490, jan. 2018. Springer Science and Business Media LLC. http://dx.doi.org/10.1007/s12206-017-1249-z.

BREUER, B.; BILL, K.H. **Bremsenhandbuch: Grundlagen, Komponenten, Systeme, Fahrdynamik**. 2. ed. Wiensbaden, DE: Vieweg & Sohn Verlag, 2004.

GILLESPIE, T. D. **Fundamentals of Vehicle Dynamics.** Warrendale: Society of Automotive Engineers, 1992.

GUERRERO, Alex; CASTILLA, Robert. Aerodynamic Study of the Wake Effects on a Formula 1 Car. Energies, [S.L.], v. 13, n. 19, p. 5183, 5 out. 2020. MDPI AG. http://dx.doi.org/10.3390/en13195183.

IGALI, Dastan; MUKHMETOV, Olzhas; ZHAO, Yong; FOK, Sai Cheong; TEH, Soo Lee. Comparative Analysis of Turbulence Models for Automotive Aerodynamic Simulation and Design. **International Journal Of Automotive Technology**, [S.L.], v. 20, n. 6, p. 1145-1152, 16 set. 2019. Springer Science and Business Media LLC. http://dx.doi.org/10.1007/s12239-019-0107-7.

JIAN, Qifei; SHUI, Yan. Numerical and experimental analysis of transient temperature field of ventilated disc brake under the condition of hard braking. **International Journal Of Thermal Sciences**, [S.L.], v. 122, p. 115-123, dez. 2017. Elsevier BV. http://dx.doi.org/10.1016/j.ijthermalsci.2017.08.013.

LIMPERT, R., **Brake Design e Safety**, 2 ed. Warrendale, SAE International, 1999.

MILLIKEN, W. F.; MILLIKEN, D. L. **Race Car Vehicle Dynamics**. Warrendale: Society of Automotive Engineers, 1995.

PANDEY, Pramod. A Higher Accuracy Exponential Method for the Numerical Solution of Second Order Elliptic Partial Differential Equations. **Journal Of Mathematical And Computational Science.** Salalah, p. 1325-1334. 27 jul. 2013.

SAE INTERNATIONAL. **RULES 2020**: Formula SAE Rules 2020. 1 ed. [S.I.]: Sae International, 2019. 136 p.

TABOREK, J. J. **Mechanics of Vehicles**. Cleveland: Penton, 1957.

VIDIYA, Manthan; SINGH, Balbir. Experimental and Numerical Thermal Analysis of Formula Student Racing Car Disc Brake Design. **Journal Of Engineering Science And Technology Review.** Manipal, p. 138-147. mar. 2017.

7. RESPONSIBILITY NOTICE

The authors are the only responsible for the printed material included in this paper